Blink characterization using curve fitting and clustering algorithms

Joseph K. Brosh[1], Ziwei Wu[2], Carolyn G. Begley[2], Tobin A. Driscoll[1], Richard J. Braun[1]

[1]Department of Mathematical Sciences, University of Delaware, Newark, USA, [2]School of Optometry, Indiana University, Bloomington, USA

Abstract

Purpose: The motion of the upper eyelid during blinking can be important in diseases and syndromes that affect the eye; these include dry eye syndrome and blepharospasm, for example. We employ mathematical methods in this proof-of-concept study to classify blink motion.
Methods: Using data from a pilot study, hypothesized lid motion functions are fit to the dynamic position of the center of the upper lid under four experimentally controlled conditions. The coefficients of these non-linear fits are used with measured data to classify blinks. Agglomerative hierarchical and spectral clustering methods were used to attempt an automatic distinction between partial and full blinks as well as between normal and abnormal blinks.
Results: Results for both approaches are similar when the input data is suitably normalized. Clustering finds outlying blinks that do not fit the model functions for lid motion well and that differ from the majority of blinks in our sample of N = 393 blinks; however, those blinks may not be outliers based on easily observed data such as blink amplitude and duration.
Conclusion: This type of analysis has potential for classifying blink dynamics from normal and pathological conditions such as recovery from Bell's palsy or dry eye syndrome, but more work is needed with larger sets of data from blinks to put forth firm conclusions.

Keywords: hierarchical clustering, spectral clustering, blinking, blink classification, dry eye

Correspondence: R.J. Braun, Department of Mathematical Sciences, University of Delaware, Newark DE 19716, USA.
E-mail: rjbraun@udel.edu

1. Introduction

During a normal eye blink, the upper lid moves inferiorly during the down phase or downstroke, and during the subsequent up phase or upstroke a thin tear film is painted over the exposed corneal and conjunctival surfaces.[1,2] The quality of the tear film left behind depends on many factors, including the speed of the lid,[3] thickness of tears under the upper lid,[4–6] total amount of tears present,[7] lipid layer dynamics,[8] and the motion of the lids themselves.[1,9,10] The dynamics of the blink have a well-known connection to the visual demands, activity level, and mental state of the subject, and blink rate is known to be altered in pathological conditions such as dry eye syndrome (DES). Thus, there may be an interplay between the effectiveness of blinks and the development of DES.[11] Other conditions that are intimately related to blinking include blepharospasm.[11]

Blinks have been categorized into three types: voluntary, reflex (*e.g.*, reactions) and spontaneous.[2,12] In a classic paper on this topic, Evinger *et al.*[12] measured the kinetics of these types of blinks using a magnetic coil search technique and skin electrodes to record the activity of the muscles involved in the blink as the eyelid opened and closed. The two main muscles involved in blinking are the orbicularis oculi muscle, which acts to close the eyelid, and the levator palpebrae, which opens the eyelid during the blink. Evinger *et al.* suggested that these muscles were aided by their associated ligaments because they act in a spring-like fashion.[12] Kaminer *et al.*[13] hypothesized that the spinal trigeminal complex plays an important role in modulating incoming neural signals to vary the blink pattern.

Blinks were also captured and analyzed by Doane[1] by filming subjects with a telephoto lens through a half-silvered mirror during the interval when the subjects believed they were relaxing before the test was to begin. He analyzed the motion of the upper lid margin by manually capturing the location in each frame and then collecting the results. He found that most blinks were partial, and that, typically, after a few partial blinks, there was a full blink. Though we often think of a full blink as when the upper and lower lids meet, it may be that most full blinks have the lids approaching each other but not necessarily touching.[14,15] It has been found via mathematical models that the lids need not touch for the fluid motion to "reset" and for there to be what is effectively a complete blink.[5,16]

A number of other studies have shown that the blink rate (BR) or interblink interval (IBI) can be affected by many factors. Reading, working on computer, or other visual tasks requiring concentration are known to decrease blink frequency,[17–20] whereas irritation or stimulation of the ocular surface increases the BR.[21–23] DES is associated with an increased BR[19,23] presumably due to the ocular surface irritation and stress provided by surface drying or increased hyperosmolarity from an unstable tear film.[24,25]

Other ocular conditions are related to blinking as well. Subjects recovering from Bell's palsy, a unilateral weakening (or sometimes paralysis) of the peripheral facial muscles, can strongly affect blinking and lead to inflammation and even functional

blindness; after one year of recovery, orbicularis oculi activity may normalize but blink amplitude may remain decreased.[26] Blepharospasm can cause rapid and involuntary blinking;[2] perhaps this and other eye distonia could be detected in a developing or less severe state so that most severe states could be avoided or limited. Grave's upper eyelid retraction has been said to have a paucity of data,[2] and more data with improved quantitative processing could aid understanding of this condition as well. In all of these cases, basic understanding could be aided by further quantification of blink processes.

Blinks occurring when the subject knows that he or she is being observed are not unconscious, but may still provide useful information. Tasks may be assigned to occupy the subjects during experiments, and this is done in the clinic either as a distraction or to study the dependence of blinks on the performed task[2,22] and stimulus type.[9,19,21] We use data from a recent pilot study by Wu *et al.*[22] in ten test subjects, including normal and DES subjects, whose blinks were recorded for one minute as part of a 2.5 minute interval. The blinks were recorded with and without a light flow from a fan blowing on the subject's eye, in each case while working on either a high- or low-concentration task. The data was taken after an initial 30 s start up phase, and the blinks were measured by monitoring the location of a centrally-located spot located near the superior lid margin. The recorded blinks were preprocessed in order to identify the start and end of blinks for each subject. The IBI was measured as the time from the maximum lid displacement of one blink to the subsequent blink. They found that even the mild stimulus from air flow used on the surface of the eye decreased the IBI and its variability regardless of whether it was a high- or low- concentration task. The high-concentration task increased IBI and its variability, and thus had an opposite effect to external stimulus. Blink amplitude, defined as the percentage of a full blink achieved at the end of the down phase of lid motion, had no significant effect from either the stimulus or task. However, they observed that the majority of blinks were partial, in accord with previous studies.[1,2,19] They also observed a difference in correlation between blink amplitude and maximum speed during the down phase depending on whether the subject was previously diagnosed with DES.

In another study by Wu *et al.*,[27] using ten normal test subjects and similar conditions, it was found that IBI regularity increased with increased flow rate from the fan providing increased surface stimulus, most likely as a protective measure. It was found that there was a roughly linear relationship between ocular surface stimulation and decrease in IBI. Because only normal subjects were used, it is possible that a different response could be present for subjects that have moderate to severe DES.

The first quantitative mathematical model of blinking of which the authors are aware was developed by Berke and Müller.[28,29] They designed a function that closely mimicked the position of the central lid margin during a blink. The function represents the displacement inferiorly, $x(t)$, from the rest position of the upper lid through the duration of the blink using:

$$x(t) = a_0 t^2 \exp(-bt^2). \tag{1}$$

There are two constants, a_0 and b, which were chosen appropriately to fit the blink amplitude and duration. This function has been modified to describe lid motion in theoretical work on tear film dynamics and blink cycles.[5,6,16] Similar functions have been implemented in theoretical models for tear film deposition for the aqueous layer alone[4,30] and including the action of polar lipids.[31–33] We shall modify this function in order to improve the fit for a wider variety of blink data, and to use those fits to classify blinks. We note that the lid motion function is not periodic in general[34] and the IBI depends on task and conditions;[2,22] in any case, we wish to study individual blinks and so Equation (1) suffices.

The purpose of this study is to develop methods to use the coefficients from a modified version of Equation (1) together with measured blink data such as amplitude and duration so that outlying blinks can be identified. If this can be done, then there is the potential to apply the method to clinical conditions like DES and Bell's palsy, among others, to quantitatively assess blinking and its relation to the condition in question. This is certain to lead to a better basic scientific understanding of conditions involving blinking, and thus has the potential to improve approaches in the clinic. We now go on to describe the methods used, then proceed to results, and finally, discussion.

2. Methods

The experimental data and methods used in this work are published elsewhere,[22,27] but for convenience we provide a brief description of them here. Then, we proceed to the mathematical approach.

2.1 Experimental measurements

For this paper, we studied $N = 393$ blinks pooled from five subjects in a recent pilot study by Wu *et al.*[22] The experimental method discussion here is closely based on that in Wu *et al.*[22] Video recordings at 250 frames per second were made of ten subjects in four conditions based on combinations of two tasks with or without a gently blowing fan. Both healthy and dry eye subjects were included in the study based on their responses to the Dry Eye Questionnaire.[35] Five subjects were chosen because they had what was judged to be the best data for lid position across all of their blinks; one subject was normal with the remaining four self-reporting dry eye symptoms. The observations were made in two different visits (one visit with a fan, one visit without). The tasks were either listening to music (low-concentration state) or playing a video game (high-concentration state). Each task lasted 2.5 min with a 15-min break between tasks. When in use, a small electronic fan was located 50 cm from the eye, resulting in a measured air speed of 1.34 mph (0.6 m/s) at the eye.This air speed is very gentle and is insufficient to move, for example, tree leaves. Subjects were seated behind a Zeiss biomicroscope system ($8\times$ magnification) with a custom-fitted camera used to record upper lid movement (Basler piA640-210 gm, Basler AG, Germany,

250 Hz). In order to track eyelid positions during blinking, a 2 mm diameter reflective white dot was centered on the margin of the right upper lid. During the visit with a fan, the recording was started one minute after the onset of air stimulus to allow subjects to become familiar with the stimulus. Only the right eye was tested and the left was held shut by the subject to ensure that stimulus from the ocular surface arose from the tested eye. Other data was collected,[22] but was not used in this work.

   The observed upper lid positions were processed as follows. When the lid appeared to start moving downward from the highest vertical position, a blink was begun. When the lid returned to that position, the blink was ended. The largest blink position for that subject without any apparent squeezing was labeled as an amplitude of 100%. A blink that did not fully close would have a blink amplitude of less than 100%. This process was repeated for each blink in the 2.5 min interval per task. This process was automated with a custom Matlab program (The MathWorks, Natick, MA, USA). We used this processed blink data in this work.

2.2 Mathematical approach

We first fit a curve to the processed lid position data. Then, the coefficients from the fitting process are combined with measured data as well as error in the fit to form a set of combined data. Then, two types of clustering are performed on the combined data.

2.2.1 Fitting the blink data

When we attempted to use Equation (1), it did not fit a significant fraction of our data well. We modified the function in Equation (1) so that the fit could be improved to better describe a larger number of blinks:

$$f(\mathbf{a}, t) = (a_0 t^2 + a_1 t^3 + a_2 t^4) \exp(-bt^c). \tag{2}$$

The parameters determined from the a non-linear least squares fit are the five quantities a_0, a_1, a_2, b, c. The special case $a_1 = a_2 = 0$ and/or $c = 2$, which includes Equation (1), were also considered. The measurement of the lid position x_i is collected at m times t_i for blink i. The vector of lid positions and times are $\mathbf{x}$ and $\mathbf{t}$, respectively; $\mathbf{f}(\mathbf{a}, \mathbf{t})$ is the vector of fitting function values at $\mathbf{t}$. m_i and varies from one blink to another, but we denote the number of time points in a particular blink as m for simplicity. For a representative case below, $m = 58$. Minimization of the sum of the square errors (SSE) over the fit parameters $\mathbf{a} = a_0, a_1, a_2, b, c$ was performed to establish the best fit for the given data via:

$$\min_{\mathbf{a}} ||\mathbf{f}(\mathbf{a}, \mathbf{t}) - \mathbf{x}||_2^2 = \min_a \sum_{i=1}^{m} [f(a, t_i) - x_i]^2 = \min_a \text{SSE}. \tag{3}$$

The resulting fit yields: $\hat{a}_i = \{\hat{a}_{0i}, \hat{a}_{1i}, \hat{a}_{2i}, \hat{b}_i, \hat{c}_i\}$, which denotes the coefficients found during the fitting for blink i. MATLAB's `lsqcurvefit` function was used for the
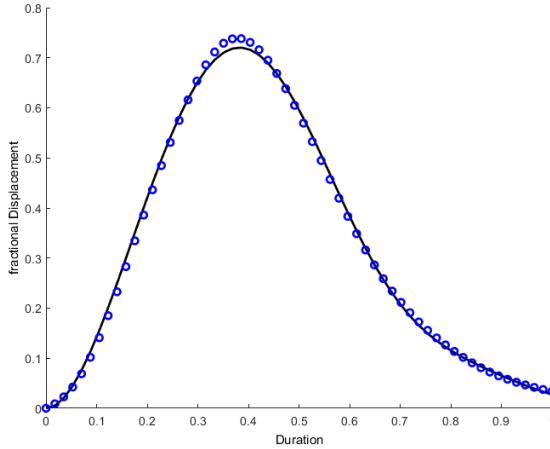
Fig. 1. An example fit of the displacement of the upper eyelid throughout the entire blink using Equation (2). The displacement fraction is relative to a representative full blink; see text for more details. The blink duration is normalized to unity for each blink for fitting.

minimization with all variables unconstrained except for c, which was limited to the interval $1 \leq c \leq 5$. The minimization and subsequent analysis was improved by normalizing the experimental data as follows. The duration of each blink was normalized to $0 \leq t \leq 1$ to allow for a more robust fit and to avoid any problems with small initial gradients in the iteration of the minimization. Furthermore, the lid displacements during the blink were renormalized by dividing by 100%, so that a fractional displacement was used rather than the percentage described in Wu *et al.*[22] Thus, a half blink would have a blink amplitude of 0.5 in our renormalized form. Using these normalizations and Equation (2), our approach frequently captured the nature of the blinks very well, with an SSE of 0.0342 and standard deviation of 0.1008 for the example shown in Figure 1 which used $m = 58$ measured displacements. It was found that most blinks had $2 \leq c \leq 3$, and as shown in Figure 2, most of the blinks with a large c value were either full blinks or blinks that Equation (2) was not able to fit well. Numerical exploration did not yield any alternative fits for the data examined, and from this evidence we assume that the fits are unique for this choice of function.

2.2.2 Clustering of the combined data

We then hypothesized that combining parameters from the fit, namely:

$$\hat{\mathbf{a}}_i = \{\hat{a}_{0i}, \hat{a}_{1i}, \hat{a}_{2i}, \hat{b}_i, \hat{c}_i\}$$

together with the log of the residual ($\ln(\text{SSE})$), and directly observed data, such as blink amplitude and duration, would result in a better classification of blinks than
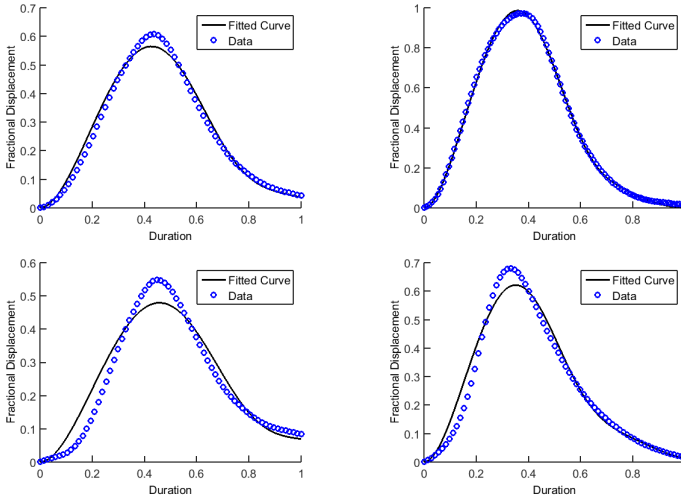
Fig. 2. Representative sample of blinks with $c \geq 3.5$.

could be obtained from using only the directly observed quantities of the blink (such as amplitude and duration). The coefficients of Equation (2) found from the fits contain some additional information about the shape of the lid displacement function compared to the blink amplitude and duration. For example, the larger positive values for c may mean faster decay back to zero displacement, but larger a_0 and a_2 could mean a steeper rise of the curve and slower decay back to zero displacement later in the blink. In what follows, we use the term "measured data" to refer to the blink amplitude (BA), blink duration (BD) and natural logarithm of the IBI (LIBI), which are recorded directly from the blinks. We use the term "fit data" to refer to the resulting coefficients from fitting Equation (2) to the observed blinks. The term "combined data" will refer to using fit data, the residual of the fit and measured data together for blinks, namely:

$$\hat{\mathbf{y}} = \left\{ \hat{a}_{0i}, \hat{a}_{1i}, \hat{a}_{2i}, \hat{b}_i, \hat{c}_i \ln(\mathsf{SSE}), \mathsf{BA}, \mathsf{BD}, \mathsf{LIBI} \right\}. \tag{4}$$

To the fit parameters, we added the logarithm of the minimum SSE, the BA, and BD (which were normalized before fitting), and the logarithm of the IBI. Altogether, we used nine quantities in $\hat{\mathbf{y}}_i$ to characterize each blink: $\{\hat{a}_{0i}, \hat{a}_{1i}, \hat{a}_{2i}, \hat{b}_i, \hat{c}_i\}$ (the fit data), the log of the residual $\ln(\mathsf{SSE}_i)$, and the three physical parameters (the measured data $\mathsf{BA}_i, \mathsf{BD}_i, \mathsf{LIBI}_i$).

We then applied hierarchical clustering methods[36,37] and spectral clustering methods[38] on the combined data. These algorithms seek to combine or cluster like data into more homogeneous groups compared to the original data, as well as to find structure in the data. By structure, we mean the ability to associate like blink displacement functions into a group and to separate unlike blinks into different

groups. After testing a variety of possibilities, we have pinpointed some promising combinations for helping to identify structure in blink data.

All blink data from the five subjects was pooled for the clustering methods; this resulted in a total of $N = 393$ blinks. Two types of clustering methods were applied to the combined data in order to group like kinds of blinks and to identify normal and outlying blinks. We begin with hierarchical clustering, and then proceed to spectral clustering.

3. Results

3.1 Agglomerative hierarchical clustering

In order to better understand the blink parameters and how they may be grouped, agglomerative hierarchical clustering was used.[37,39] In this method, the number of clusters is set in advance; we varied the number of clusters subjectively to get the best results. More details of this approach are given in Appendix A. The clustering was initially performed on only the three measured parameters that can be observed directly without using any curve fitting (BA_i,BD_i,ln(IBI_i)); the results for the three clusters are shown in Figure 3. For this clustering, we employed a Scaled-Euclidean metric with a weighted average linkage, which normalizes the data and improves the results. Three clusters were readily identified, corresponding to short partial blinks with with approximately less than 40% closure; forced, fuller blinks with long duration and more than 70% closure; and "normal" blinks as shown in Figure 3. It was found that when using agglomerative hierarchical clustering on the combined set of all observed and fit parameters $\hat{\mathbf{y}}$ without prior normalization, no discernible groups emerged for any combination of metric or linkage discussed in the appendix. However, the results were improved when each component of the data was normalized with its z-scores; those results are shown together with the spectral clustering results below.

3.2 Spectral clustering

Some details of spectral clustering[38] are given in Appendix B. When we perform spectral clustering, we consider all of the combined data $\hat{\mathbf{y}}$. To facilitate a better clustering, all of the data of each factor x was normalized to its z-score via:

$$\mathbf{z}^{(k)} = \frac{\mathbf{x}^{(k)} - \bar{x}^{(k)}\mathbf{1}}{s^{(k)}\mathbf{1}}, \tag{5}$$

where $\mathbf{x}^{(k)}$ contains the set of the k-th variable of the combined data (*e.g.*, the blink durations), $\mathbf{z}^{(k)}$ contains the corresponding z-scores, $\bar{x}^{(k)}$ is the mean of the k-th variable (a scalar), $\mathbf{1}$ is a vector with unit entries that is the same size as $\mathbf{x}^{(k)}$, and $s^{(k)}$ is the standard deviation of the k-th variable (a scalar).
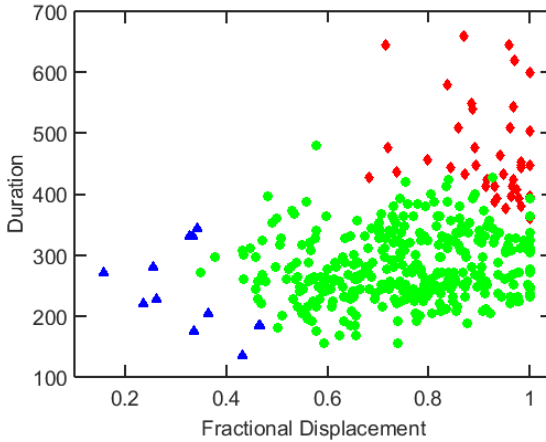
Fig. 3. Clustering performed using only the physical parameters: amplitude, duration, and $\ln(\text{IBI})$, with a Scaled-Euclidean distance and a weighted similarity metric. The clusters are shown using duration and fractional displacement axes only, although the remaining variable $\ln(\text{IBI})$ also affects the clustering.

Plotting a_0, a_1 and a_2 from the fit data shows that most of the blinks appear to lie on a crescent-like curve after normalization to the z-scores (Fig. 4). We hypothesize from this result that we may call a blink "normal" if it lies close to this curve. We did not determine an analytical approximation to this curve. For smaller values of a_0 and a_2, and larger values of a_1, the blink fits are more scattered and lie relatively far from the curve; we hypothesize that these blinks are outliers. Spectral clustering shows that the blinks that are more scattered are clustered in terms of the nine clustering quantities. This is indicated by the lighter-colored circles where the circles are scattered from the curve.

Some of the blinks hypothesized as outliers are shown in Figure 5. Most of these outliers are either short, partial blinks, or blinks that have irregular positions as functions of time, or both. In addition, we also note that blinks from Subject 4, when performed without a fan blowing and while listening to music, had much larger blink amplitude and longer duration than the other subjects. This could be due to an underlying physiological problem, and would require further review; there is too little data to draw a conclusion here.

The values assigned to the nodes by the spectral clustering can be determined by the number of clusters given to the k-means clustering algorithm at the end of the spectral clustering algorithm.[38] The results for four different choices of cluster number are shown in Figure 6. From the figure, we see that as the requested number of clusters increases, we are able to capture more subsets of the scattered results that do not appear to lie on the crescent-shaped curve in the coefficient plot.

After normalizing all combined data to their z-scores, we see that similar results
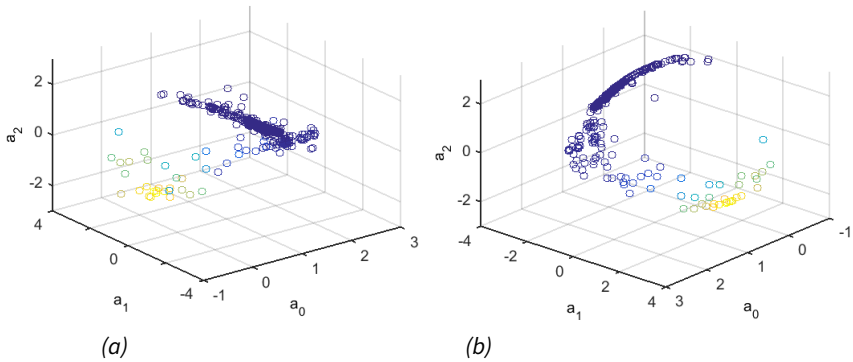
Fig. 4. Spectral clustering performed using all physical and fit parameters displayed using the three polynomial coefficients of the fit normalized to their z-scores. Plot *(b)* is the same as plot *(a)*, except that the viewpoint has been rotated $180°$ about the a_2 axis. Note that even though Figure 4 is shown with only three of the blink features (from fit data), all nine of the combined data are used in the spectral clustering. The points are colored using the eigenvector corresponding to the second smallest eigenvalue.

are obtained when comparing the agglomerative clustering (right) to the spectral clustering (left) in Figure 7. This agglomerative clustering was performed using a cosine metric with a weighted average linkage and three clusters. In addition, we see that the spectral clustering is able to identify subgroups (when increasing the number of clusters given to k-means) that the agglomerative clustering cannot. In particular, the clearest results came from seeking three clusters from the agglomerative clustering, while more clusters appeared from spectral clustering (at least six clear ones) and some of the spectral clusters had very few members. In either case, the largest cluster had a_2 very close to zero or larger (roughly $a_2 \geq 0$), with the other clusters appearing largely for $a_2 < 0$. Because different approaches to clustering give a similar result for the biggest cluster, we believe that this supports our hypothesis about detection of normal blinks via our approach.
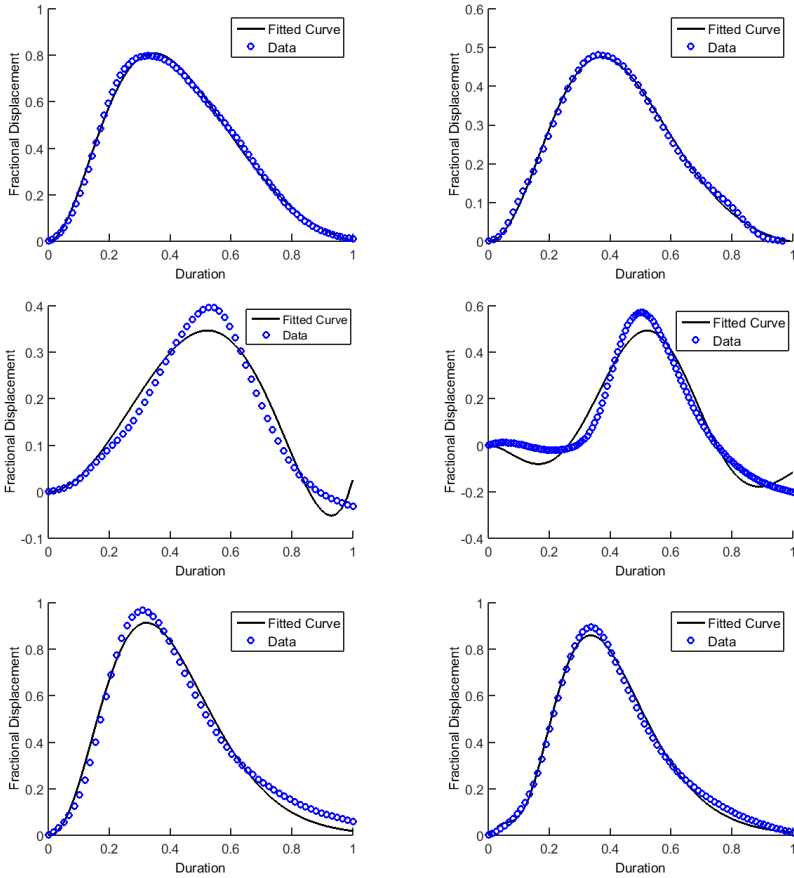
Fig. 5. A representative sample of the plots of the blinks that were outliers found from spectral clustering.
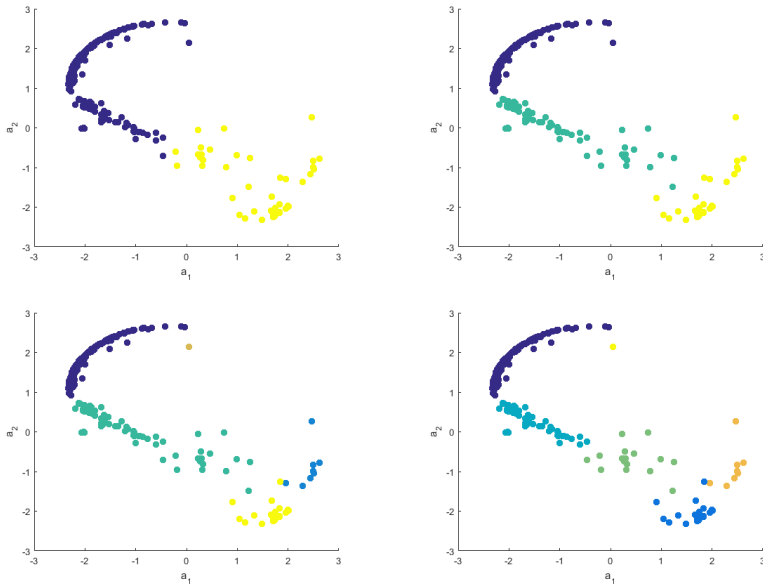
Fig. 6. Plots of the clusters found using spectral clustering with two (top left), three (top right), five (bottom left), and six (bottom right) clusters. The use of five and six clusters was shown instead of four and five because of the identified singleton cluster near the top of the bottom two figures.
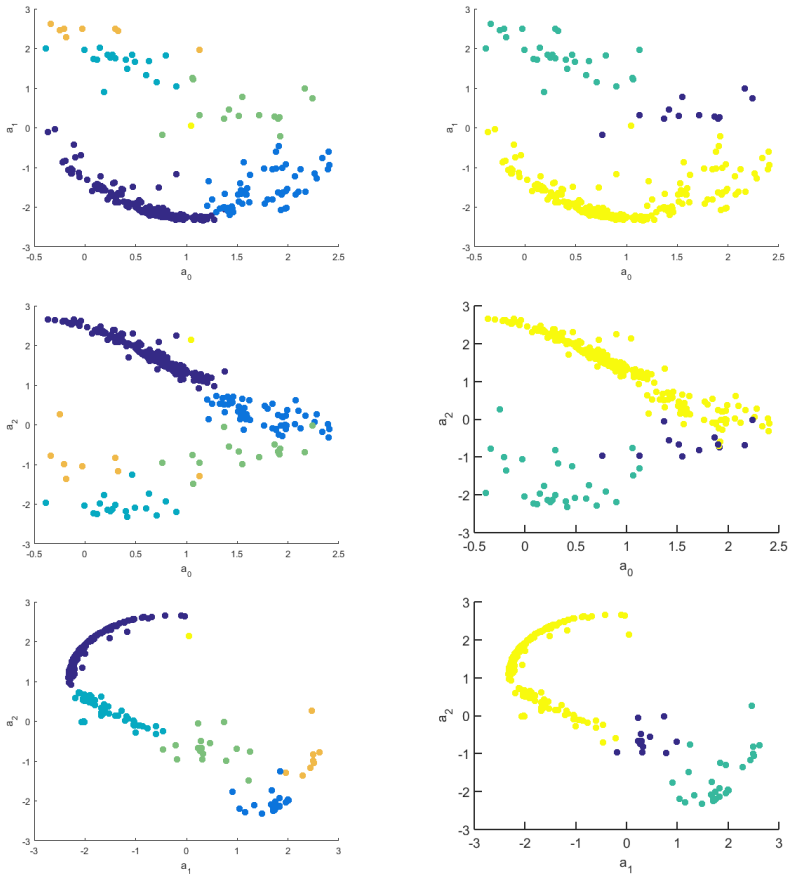
Fig. 7. Plots of the clustering comparing both the results from the spectral and agglomerative methods. The left column corresponds to spectral clustering; the right, to agglomerative clustering. Each row is a different view of the result; note the axis labels. All of the combined parameters were normalized to their z-scores prior to clustering.

Spectral clustering uses more features and produces more differentiation between the points, particularly among the outliers. If we select the blinks corresponding to the yellow cluster in the top right plot in Figure 6, a group starts to form around a blink amplitude of 0.6 and blink duration of 300 ms, one that is not easily distinguished using the clusters based on measured data alone (Fig. 8).

The number of outlying blinks from the pooled blink set are shown by subject and task in tabular form (Table 1). By subject, three of the subjects account for the vast majority of the outlying blinks from the spectral clustering method for either threshold value. The outliers are in the the green, brown, and bright blue clusters in the bottom right plot in Figure 6 and the yellow cluster in the top right plot in Figure 6. By task, outlying blinks appeared to be associated with the fan stimulus for either threshold value. For both cluster selections, it was found that the music tasks accounted for 75% and 76% of the total outliers, respectively. This finding agrees with previous results.[19,22]

Table 1. (a) Table of the number of outliers according to the specific subject (Sub) and task for the yellow cluster in the top right plot in Figure 6. *(b)* Table of the number of outliers according to the specific subject and task for the yellow cluster in the top left plot in Figure 6. The total for each task and subject is given in the last column and row of each table, respectively.

	Sub 1	Sub 2	Sub 3	Sub 4	Sub 5	Total
Fan & Game	1	0	2	1	1	5
Fan & Music	1	1	3	2	0	7
No Fan & Game	0	0	2	0	0	2
No Fan & Music	0	4	7	3	0	14
Total	2	5	14	6	1	28

(a)

	Sub 1	Sub 2	Sub 3	Sub 4	Sub 5	Total
Fan & Game	2	2	2	1	1	8
Fan & Music	3	1	6	2	0	12
No Fan & Game	0	0	2	0	0	2
No Fan & Music	0	7	10	3	0	20
Total	5	10	20	6	1	42

(b)

We also see that Subjects 4 and 5 have the least number of outliers (six and one, respectively), and for both subjects, changing the thresholding eigenvalue does not add in any new outliers. We can also identify that the task where subjects do not listen to music and play a video game does not produce any new outliers between the thresholds. Additionally, using Table 1, we can see that Subject 3 has the most outliers for both eigenvalues used.

4. Discussion

After normalizing the blink duration to be $0 \leq t \leq 1$, we found that any blinks with a c value outside of the interval of roughly $1.5 < c < 3$ can be considered outliers in this dataset. From Figure 2, we see that blinks with a $c \gtrsim 3.5$ are normally very full blinks that reach their maximum displacement of the upper lid very quickly, and then take longer than normal to reopen. From Doane's study,[1] the average downstroke time was 82 ms and the average upstroke time was 176 ms, but Evinger *et al.*[12] found a range of blink amplitudes and durations with a non-linear relationship between them. The approach here includes both observed data like BA and BD as well as fit data â, and thus, additional information about how the blink trace is shaped. For the same BA and BD, different functions can achieve those same observed quantities, but they may be separated if the fit data â are included. Figure 8 shows that many of the outliers appear in what looks like normal blink amplitude and duration ranges. These outliers may have relatively slow and linear downstrokes, or other features that are unusual in the shape of the blink trace. Including this information has resulted in a more automatic identification of blink traces that fell outside the normal range for this dataset.

Spectral clustering may provide the best option for additional classification. It appears that most blinks lie on a crescent-like curve in the polynomial coefficient space (Fig. 4). The outliers in Figure 4 appear to consist mostly of blinks short, partial blinks, as well as a few with irregular shapes. By selecting a particular eigenvalue threshold, we are able to determine a cutoff as to what could be considered outliers in a given dataset.

Using this criteria for the cutoff, when we overlay the outliers from spectral clustering we are able to identify a potential grouping of blinks (Fig. 8) that differs from the majority. Spectral clustering using the parameters from curve fitting together with the measured physical values allowed for an additional classification not possible by the agglomerative clustering using only the physical values.

The number of subjects was small in this study, so general conclusions about blinking and task or disease are not advisable. However, given that the blink rate is known to vary widely with task, mental state, and disease, these methods show great potential for understanding the effects of these different conditions on blinking.
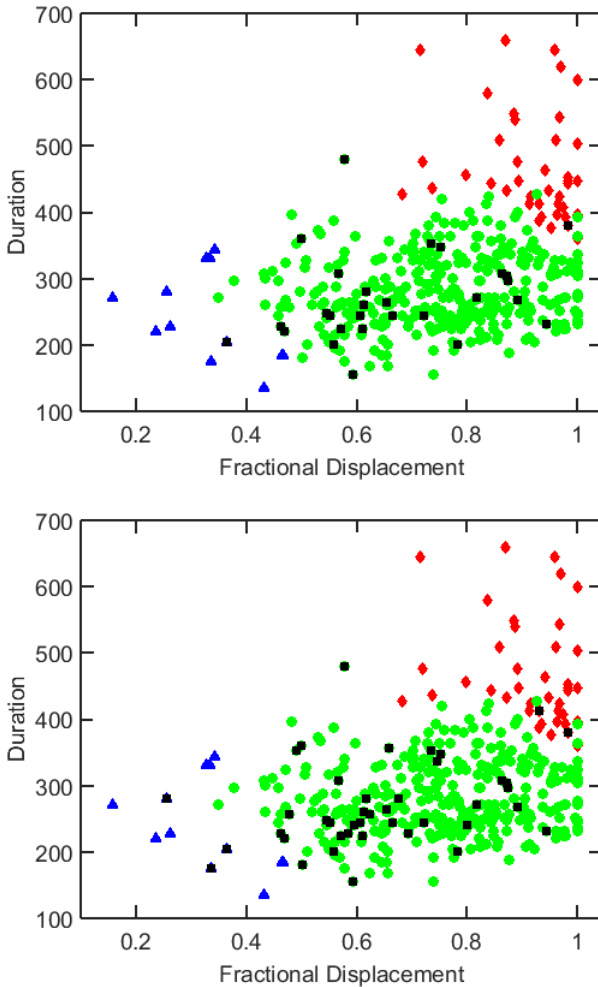
Fig. 8. Plot of the groups found from the agglomerative clustering (red, green, blue) with out-liers as determined by spectral clustering (black) superimposed. The top figure corresponds to the yellow cluster in the top right plot in Figure 6, while the bottom one corresponds to the yellow cluster in the top left plot in Figure 6.

5. Conclusion and future directions

A refined classification of blinks was possible through the use of combined data that used both measured data and fit parameters indicates the possibility of identifying abnormal blinks and perhaps other conditions such as DES.[22] Further work with a larger set of subjects and more blinks per subject could verify our conjecture about the possible classification of blinks using data from both measured and fit parameters. More data may allow the study of subject-specific classification, which can be desirable in some cases,[22] but was not feasible here. More data in condition-specific contexts such as Bell's palsy or blepharospasm may also be aided by a more automated classification of blinks.

We note that clustering results depend on the techniques chosen and the judgment of the user.[36] We have been able to obtain similar results from distinct clustering methods provided that each component of the combined data is normalized to its z-scores. Using this normalization may make the results more robust between methods, but work with more data is needed.

Our approach is limited to some extent by our choice of blink displacement function. We showed some of the worst case fits in Figure 2, and thus other functions or approaches to the fits may work for some blinks.[40]. Furthermore, we only used a summary of the curves by using the fit coefficients rather than the functions themselves; using clustering on the functions themselves may yield additional insights.[41] Additionally, other clustering approaches such as those found in the statistical software R maybe be appropriate.

To summarize, blink frequency (or equivalently, IBI) is currently the most common parameter used to categorize blinking in normals and various disease states, but blink frequency does not directly describe the action of the blink itself. There are many blink parameters (blink amplitude, velocity, etc.) that have been studied, but examination of individual parameters are unlikely to adequately describe the blinking process due to the complex interactions among them. Therefore, the analytical method we suggest here has the advantage of taking into account a greater number of the many parameters and quickly identifying groups of similar blinks and outliers. This quantitative method has potential for identifying blinks that may be characteristic of various disease states, and possibly, quantifying the effect of treatments if the treatment is designed to restore normal blinking. In the field of dry eye, there is a current emphasis on neuropathic causes for the condition. Given that the blinking and tear response as well as the symptoms all arise from sensory neurons at the ocular surface, blinking may be a reasonable endpoint for testing the ocular surface neural response.[42] Additional directions could involve combining blink motion observations with physiological measurements of muscle activity (such as orbicularis oculi or levator palpebrae superioris muscles)[2] may help clarify at least some causes of variations in blink activity. Similarly, including appropriate neural activity may also shed light on connections between abnormal blinks and neural control of blinking.[9,12,21,26,43,44]

Acknowledgments

A. Agglomerative hierarchical clustering

Agglomerative clustering can be thought of as a method for starting with a binary tree of data that is merged into groups of similar points successively. To perform this type of clustering, we require two main inputs besides the data. One is a specified distance metric between any two data points and a measure of similarity between all the groups of data points. For clustering algorithms, some specific distance metrics are often employed, *i.e.*:

Euclidean metric	$d(x,y) = \sqrt{\sum_{i=1}^{n}(x_i - y_i)^2}$
Scaled-Euclidean metric	$d(x,y) = \frac{1}{\max[d(x,y)]}\sqrt{\sum_{i=1}^{n}(x_i - y_i)^2}$
Chebyhev metric	$d(x,y) = \max_{i}(|x_i - y_i|)$
Cosine metric	$d(x,y) = 1 - \frac{\mathbf{x}\cdot\mathbf{y}}{||\mathbf{x}||\,||\mathbf{y}||}.$

It should be noted that the cosine metric is not strictly a metric in the classical sense (the triangle inequality does not hold). Generally speaking, a Euclidean distance metric is most favorable for low-dimensional datasets where the range of distances only goes over a few orders of magnitude. For higher dimensional datasets, or ones with a wide range of distances, a Scaled-Euclidean metric is normally preferred. The Chebyshev distance is normally appropriate when the difference between any two points is better represented by the differences in individual dimensions rather than all of the dimensions together. The cosine metric works well when trying to capture the similarity between certain feature changes in multiple dimensions.

Once a distance metric is chosen, the next thing to determine is the linkage between each group. Linkage is, in a sense, a measure of how similar two groups are to one another. There are multiple kinds of linkages that are often used in this type of clustering method; let r be a cluster formed by combining two clusters p and q, and let $x_i^{(r)}$ be the i-th element in cluster r, and let $\mathrm{dist}(x,y)$ be a specified distance metric.

Some common linkages are as follows:

$$\text{Single} \qquad d(r, s) = \min_{i,j}[\text{dist}(x_i^{(r)}, x_j^{(s)})] \qquad (6)$$

$$\text{Complete} \qquad d(r, s) = \max_{i,j}[\text{dist}(x_i^{(r)}, x_j^{(s)})] \qquad (7)$$

$$\text{Average} \qquad d(r, s) = \frac{1}{n_r n_s} \sum_{i=1}^{n_r} \sum_{j=1}^{n_s} \text{dist}(x_i^{(r)}, x_j^{(s)}) \qquad (8)$$

$$\text{Weighted Average} \qquad d(r, s) = \frac{d(p, s) + d(q, s)}{2} \qquad (9)$$

Here, the weighted average linkage is special, in that it is recursively defined by the average of linkages $d(p, s)$ and $d(q, s)$ between previously computed clusters p, q, and s.

It should be noted that agglomerative clustering is not a fully automatic clustering scheme; the distance metric, group linkage, and number of clusters must be specified.

For the agglomerative clustering used in this paper, after selecting a desired metric to use, the distances were computed using MATLAB's `pdist` function, which uses one of the metrics specified from the above list, where each column of the data matrix represents a different dimension. Then MATLAB's `linkage` function was used to determine the similarity between any two groups, using one of the specified methods above. Once the distances and linkage were computed, a predefined number of clusters was computed by MATLAB's `cluster` function. The number of desired clusters was varied until discernable groups emerged, with a recalculation of `cluster` performed at every step.

B. Spectral clustering

Unlike agglomerative clustering, where a distance metric, linkage weighting, and number of clusters must be specified, spectral clustering is, in a sense, completely automated, and one does not specify this parametric information.[38] (We include the latter reference as a particularly accessible treatment.) We suppose that there are n blinks. To perform spectral clustering, we first calculate the Euclidean distance matrix:

$$\mathbf{G} = (g_{ij}), \text{ with elements } g_{ij} = ||\mathbf{x}_i - \mathbf{x}_j||_2^2 \qquad (10)$$

where:

$$||\mathbf{x}_i - \mathbf{x}_j||_2 = \left[\sum_{m=1}^{n} \left(x_i^{(m)} - x_j^{(m)} \right)^2 \right]^{1/2} \qquad (11)$$

is the standard 2-norm for vectors $\mathbf{x}$ with n components per blink. Here i and j denote different blinks with $i = 1, 2, \ldots, N$ and $j = 1, 2, \ldots, N$; the superscript (m) denotes the component of the vector of data for a specific blink with $m = 1, 2, \ldots, n$. In our

case, we used a vector of $n = 9$ components corresponding to the measured and fit parameters for each blink.

We then exponentiate the elements of the distance matrix to obtain the similarity matrix $\mathbf{W}$ with elements:

$$w_{ij} = e^{-2g_{ij}}. \tag{12}$$

The similarity matrix W represents a local distance distribution, *i.e.*, the points that are closest together will have a stronger influence on each other than points that are far away. We also define the diagonal degree matrix D whose diagonal elements are:

$$d_{ii} = \sum_{j=1}^{N} w_{ij}, \tag{13}$$

for N blinks. The degree matrix D represents how strongly connected each data point is to every other data point. We then form the normalized graph Laplacian:

$$L = I - D^{-\frac{1}{2}} W D^{-\frac{1}{2}}, \tag{14}$$

where I is the identity matrix. We now calculate the eigenvalues of L and sort them in increasing order. Zero is always an eigenvalue of L; the geometric multiplicity of the zero eigenvalue indicates the number of connected components of the theoretical graph of the data (in the sense of graph theory).[38] The connected components are then taken to be the clusters. One then uses the associated eigenvectors to assign each point to a cluster. To do this, say that the zero eigenvalue is repeated and has k independent eigenvectors, *i.e.*, its geometric multiplicity is k. The k eigenvectors associated with the zero eigenvalue are assembled into a matrix with each row representing a data point, and each row of the matrix suitably normalized.[38] Then, K-means clustering[37] is applied to obtain k clusters from this normalized data. The resulting clusters are the output of the spectral clustering algorithm.

There are different interpretations of the spectral clustering approach that may help visualize what is happening. One is that this process can be thought of as an approximation to the certain minimization problems on graphs, which are variations of the mincut problem. The conversion of the clustering problem to the graph cut problem has the advantage of being automatic in the sense that the algorithm determines the number of clusters from the data. Another is to think of the probability of being at various points on a graph due to random hopping by a flea (*i.e.*, a random walk model for diffusion). If a flea jumps around the nodes of a network, with probabilities of jumps scaled to the distance between nodes, then spectral clustering simulates the diffusion of probability of being at every node. The idea is that the flea jumps between clusters rarely, so the clusters get separated in probability depending on where the flea starts. Mathematically, the uniform probability (a steady state in diffusion) is the constant function over the graph, which is always an eigenvector of eigenvalue zero. The initial position of the flea gets projected onto the eigenvectors. If there are k "natural" clusters, then there will be k eigenvectors with eigenvalues much closer to zero than all of the others.

References

1. Doane MG. Interaction of Eyelids and Tears in Corneal Wetting and the Dynamics of the Normal Human Eyeblink. Am. J. Ophthalmol. 1980;89, 507–516.

2. Cruz AAV, Garcia DM, Pinto CT, Cechetti SP. Spontaneous Eyeblink Activity. Ocul. Surf. 2011;9, 29–30.

3. Wong H, Fatt I, Radke C. Deposition and thinning of the human tear film. J. Colloid Interface Sci. 1996;184, 44–51.

4. Jones MB, Please CP, McElwain DLS, Fulford GR, Roberts AP, Collins MJ. Dynamics of tear film deposition and draining. Math. Med. Biol. 2005;22, 265–88.

5. Heryudono A, Braun R, Driscoll TA, Cook L, Maki KL, King-Smith PE. Single-Equation Models for the Tear Film in a Blink Cycle: Realistic Lid Motion. Math. Med. Biol. 2007;24, 347–77.

6. Deng Q, Braun RJ, Driscoll TA. Heat transfer and tear film dynamics over multiple blink cycles. Physics of Fluids, 2014;26(7): 071901.

7. Palakuru J, Wang J, Aquavella J. Effect of Blinking on Tear Dynamics. Invest. Ophthalmol. Vis. Sci. 2007;48, 3032–7.

8. Braun RJ, King-Smith PE, Begley CG, Li L, Gewecke NR. Dynamics and function of the tear film in relation to the blink cycle. Prog. Retin. Eye Res. 2015;45, 132–164.

9. Manning KA, Evinger C. Different Forms of Blinks and Their Two-stage Control. Exp. Brain Res. 1986;64, 579–588.

10. Korb DR, Baron DF, Herman JP, Finnemore VM, Exford JM, Hermosa JL, et al. Tear Film Lipid Layer Thickness as a Function of Blinking. Cornea, 1994;13, 354–59.

11. Evinger C, Bao J, Powers A. Dry eye, blinking, and blepharospasm. Mov. Disc. 2002;17, 75–78.

12. Evinger C, Manning KA, Sibony PA. Eyelid Movements. Mechanisms and Normal Data. Invest. Ophthalmol. Vis. Sci. 1991;32, 387–400.

13. Kaminer J, Powers A, Horn KG, Hui C, Evinger C. Characterizing the Spontaneous Blink Generator: An Animal Model. J. Neurosci. 2011;31, 11256–11267.

14. Korb DR, Blackie CA, McNally EN. Incomplete blinking: Exposure keratopathy, lid wiper epitheliopathy, dry eye, refractive surgery, and dry contact lenses. Cont. Lens Ant. Eye, 2007;30, 37–51.

15. Pult H, Korb DR, Murphy PJ, Riede-Pult BH, Blackie CA. A new model of central lid margin apposition and tear film mixing in spontaneous blinking. Cont. Lens Ant. Eye, 2015;38, 173–180.

16. Deng Q, Braun RJ, Driscoll TA, King-Smith P. A model for the tear film and ocular surface temperature for partial blinks. Interfacial Phenom. Heat Transf. 2013;1(4): 357–381.

17. Acosta MC, Gallar J, Belmonte C. The influence of eye solutions on blinking and ocular comfort at rest and during work at video display terminals. Exp. Eye Res. 1999;68, 663–669.

18. Cardona G, Garcia C, Seres C, Vilaseca M, Gispets J. Blink rate, blink amplitude, and tear film integrity during dynamic visual display terminal tasks. Curr. Eye Res. 2011;36, 1909–197.

19. Himebaugh N, Begley C, Bradley A, Wilkinson J. Blinking and tear break-up during four visual tasks. Optom. Vis. Sci. 2009;86(2): 106–114.

20. Schlote T, Kadner G, Freudenthaler N. Marked reduction and distinct patterns of eye blinking in patients with moderately dry eyes during video display terminal use. Graefes Arch. Clin. Exp. Ophthalmol. 2004;242, 306–312.

21. Nakamori K, Odawara M, Nakajima T, Mizutani T, Tsubota K. Blinking is controlled primarily by ocular surface conditions. Am. J. Ophthalmol. 1997;124, 24–30.

22. Wu Z, Begley CG, Situ P, Simpson T, Liu H. The Effects of Mild Ocular Surface Stimulation and Concentration on Spontaneous Blink Parameters. Curr. Eye Res. 2014;38(1): 9–20.

23. Tsubota K, Hata S, Okusawa Y, Egami F, Ohtsuki T, Nakamori K. Quantitative videographic analysis of blinking in normal subjects and patients with dry eye. Arch. Ophthalmol. 1996;114, 715–720.

24. Liu H, Begley C, Chen M, Bradley A, Bonanno J, McNamara NA, et al. A Link between Tear Instability and Hyperosmolarity in Dry Eye. Invest. Ophthalmol. Vis. Sci. 2009;50, 3671–79.

25. Begley CG, Simpson T, Liu H, Salvo E, Wu Z, Bradley A, et al. Quantitative analysis of tear film fluorescence and discomfort during tear film instability and thinning. Invest. Ophthalmol. Vis. Sci. 2013;54, 2645–2653.

26. Vanderwerf F, Reits D, Smit AE, Metselaar M. Blink Recovery in Patients with Bells Palsy: A Neurophysiological and Behavioral Longitudinal Study. Invest. Ophthalmol. Vis. Sci. 2007;48, 203–213.

27. Wu Z, Begley CG, Situ P, Simpson T. The Effects of Increasing Ocular Surface Stimulation on Blinking and Sensation. Inv. Ophth. & Vis. Sci. 2014;55(3): 1555–1563.

28. Berke A, Mueller S. Einfluss des lidschlages auf die Kontaktlinse und die zugrundeliegenden Kräfte. die Kontaktlinse, 1996;1, 17–26.

29. Berke A, Mueller S. The kinetics of lid motion and its effects on the tear film. Lacrimal Gland, Tear Film, and Dry Eye Syndromes 2. Ed. by DA Sullivan, DA Dartt, MA Meneray. New York: Plenum, 1998; 417–424.

30. Jossic L, Lefevre P, Loubens C de, Magnin A, Corre C. The Fluid Mechanics of Shear-thinning Tear Substitutes. J. Non-Newtonian Fluid Mech. 2009;61, 1–9.

31. Jones MB, McElwain DLS, Fulford GR, Collins MJ, Roberts AP. The effect of the lipid layer on tear film behavior. Bull. Math. Biol. 2006;68, 1355–81.

32. Aydemir E, Breward CJW, Witelski TP. The effect of polar lipids on tear film dynamics. Bull. Math. Biol. 2010; 1–31.

33. Zubkov V, Breward CJW, Gaffney EA. Coupling Fluid and Solute Dynamics Within the Ocular Surface Tear Film: A Modelling Study of Black Line Osmolarity. Bull. Math. Biol. 2012;74, 2062–2093.

34. Ponder E, Kennedy WP. On the Act of Blinking. Quart. J. Exp. Physiol. 1928;18, 89–110.

35. Begley CG, Chalmers RL, Abetz L, Venkataraman K, Mertzanis P, et al. The relationship between habitual patient-reported symptoms and clinical signs among patients with dry eye of varying severity. Invest. Ophthalmol. Vis. Sci. 2003;44, 4753–4761.

36. Estivill-Castro V. Why So Many Clustering Algorithms? A Position Paper. ACM SIGKDD Explorations Newsletter, 2002;4(1): 65–75.

37. Everitt B. Cluster Analysis. 5th. Chichester, West Sussex, UK. Wiley, 2011;

38. Luxburg U von. A Tutorial on Spectral Clustering. Stat. Comput. 2007;17, 395–416.

39. Johnson SC. Hierarchical Clustering Schemes. Psychometrika, 1967;32, 241–254.

40. Ramsay JO, Silverman BW. Functional Data Analysis. 2nd. Berlin. Springer, 2005;

41. Jacques J, Preda C. Functional Data Clustering: A Survey. Adv. Data Anal. Class. 2014;8, 231–255.

42. Rosenthal P, Borsook D. Ocular Neuropathic Pain. Br. J. Ophthalmol. 2016;100, 128–134.

43. Belmonte C, Gallar J. Cold Thermoreceptors, Unexpected Players in Tear Production and Ocular Dryness Sensations. Invest. Ophthalmol. Vis. Sci. 2011;52, 3888–3892.

44. Parra A, Gonzalez-Gonzalez O, Gallar J, Belmonte C. Tear fluid hyperosmolality increases nerve impulse activity of cold thermoreceptor endings of the cornea. Pain, 2014;155, 1481–1491.